

Numerical Modeling for Different Types of Fractures

Xiaoqin Cui*, CREWES, Department of Geoscience University of Calgary, Canada
xicui@ucalgary.ca
and

Laurence R. Lines, Edward S. Krebs, Department of Geoscience, University of Calgary, Canada

Abstract

Research has shown that fractures can be modeled as a non-welded contact (linear slip) interface. Therefore, in the long wavelength limit, fractured homogeneous isotropic media are equivalent to transversely isotropic media (TI). The azimuthal anisotropic parameters (Thomsen, 1986) are related to the fracture character parameters: tangential and normal compliances. A group theory calculation (Schoenberg and Muri, 1989) was extended to calculate the elastic moduli of a fractured medium that the non-welded contact interface is not approach to zero. In this paper, seismic wave propagation is affected by properties of the fractures in three different cases: horizontal, vertical and tilted fractures embedded in a homogeneous isotropic medium. We illustrate the response of the fracture thickness in the synthetic seismograms in each case later on.

Introduction

The upper crust of the earth is considerably layered with complex geometry interfaces between layers with different elastic parameters as well as a single thin layer medium with a unique elastic parameter. The two half spaces in the limit of the interface are either in perfectly welded contact or imperfect non-welded contacts. The imperfect non-welded contact interfaces are possibly formed due to artificial or natural unbalanced compressions and tensions exerted on the medium, Thus there are non-unique patterns such as horizontal, vertical and tilted fractures. The non-welded contact interfaces are embedded in background media, and these types of the geological structures, are known as joints, fractures and faults, depending upon the length and the width of the interface. In general understanding, the non-welded contact interface separates geological formations into two side spaces, and forms an anisotropic media, in which fast and the slow shear waves propagate, that are orthogonally polarized to each other (Crampin, 1986). However, the width of the fracture is normally less than 10cm, so that it is difficult to detect the fracture structure with typical frequencies of the seismic waves (Lines et al, 2008). Regardless of the seismic resolution, it is still hard to indicate the fracture structure in a homogeneous isotropic medium because there is no impedance contrast around the fracture. In 1980, Schoenberg in his pioneering work produced a theory that a fracture is modeled as a non-welded contact linear slip interface, where the particle displacements are the discontinuous across interface and the stresses are continuous across it. Additionally, the particle displacements are linearly proportional to the stresses. Pyrak-Nolte (1990) has confirmed non-welded contact interface theory by laboratory measurements. In 2000, Slawinski and Krebs used the 2D generalized homogeneous approach to model SH and P-SV wave propagation in nonwelded contact interface as a horizontal fracture

Theory and Methods

Schoenberg and Muir (1989) presented the group theory formula based on the effective medium theory (Backus, 1962) to conveniently calculate the elastic moduli for the fractured and unfracture media. Consider homogeneous media that are layered and perfectly bonded (Figure 1) to form the block layered medium. Let the block layered medium thickness, H , be smaller than the minimum wavelength, and perpendicular to the vertical axis Z . It includes n constituent isotropic layers, $i=1, 2, \dots, n$. Respect to

the block of the layered medium H , each thin constituent has an individual thickness H_i and a relative thickness $h_i = H_i/H$. Under the long wavelength assumption, once the thickness and impedance of a thin constituent approaches zero, the behavior of the layered medium blocks are the same as transverse isotropic medium, where homogeneous media combine with the non-welded contact linear slip interfaces paralleled to horizontal axis X (Schoenberg, 1980). In Hooke's Law, the relationships of the stress σ_{ji} , elastic modulus c_{jk} and strain ε_{ki} for i -th constituent can be written as $\sigma_{ji} = \sum_{k=1}^6 c_{jk} \varepsilon_{ki}$ $j=1 \dots 6$; $i=1 \dots n$.

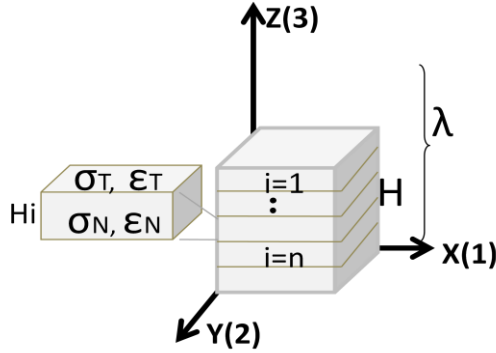


Figure 1: Block of the layered media

$$\begin{bmatrix} \sigma_1 \\ \sigma_2 \\ \sigma_6 \\ \sigma_3 \\ \sigma_4 \\ \sigma_5 \end{bmatrix} = \begin{bmatrix} \begin{matrix} c_{11} & c_{12} & 0 \\ c_{21} & c_{22} & 0 \\ 0 & 0 & c_{66} \end{matrix} & \begin{matrix} c_{13} & 0 & 0 \\ c_{23} & 0 & 0 \\ 0 & 0 & 0 \end{matrix} \\ \begin{matrix} c_{31} & c_{32} & 0 \\ 0 & 0 & 0 \\ 0 & 0 & 0 \end{matrix} & \begin{matrix} c_{33} & 0 & 0 \\ 0 & c_{44} & 0 \\ 0 & 0 & c_{55} \end{matrix} \end{bmatrix} \begin{bmatrix} \varepsilon_1 \\ \varepsilon_2 \\ \varepsilon_6 \\ \varepsilon_3 \\ \varepsilon_4 \\ \varepsilon_5 \end{bmatrix}$$

$\sigma_N = \overline{c_{NT}} \varepsilon_T + \overline{c_{NN}} \varepsilon_N \Rightarrow \sigma_{Nf} \approx \overline{c_{NNf}} \varepsilon_{Nf}$

Figure 2: Matrix expression for Hooke's Law

The matrix expression presents the relationship of stress and strain for the transverse isotropy medium with vertical symmetrical axis (VTI). The square with dashed lines divides the stiffness matrix c_{jk} into 4 stiffness sub-matrixes c_{TT} , c_{TN} , c_{NT} and c_{NN} . Where c_{NT} is the transpose of corresponding c_{TN} (Schoenberg and Muir, 1989). Following Backus's theory (1962), the layered media are parallel to the horizontal axis $x(1)$ (Figure 1) and it is assumed that all of the stress components acting on the paralleled to layering planes are the same in all layers in the media, i.e., $\sigma_3 = \sigma_{33i}$, $\sigma_4 = \sigma_{23i}$, $\sigma_5 = \sigma_{13i}$. $i=1 \dots n$. And all strain components acting in the plane of the layering are the same in all layers over thickness H , i.e. $\varepsilon_1 = \varepsilon_{11i}$, $\varepsilon_2 = \varepsilon_{22i}$, $\varepsilon_6 = 2\varepsilon_{12i}$. $i=1 \dots n$. The other stress and strain components i.e. σ_1 , σ_2 , σ_6 and ε_3 , ε_4 , ε_5 are different from layer to layer, to calculate an average value will be taken to use as the constant value within a layer. Also the weighted average value of the thickness will be the value for the total value over full thickness H (Schoenberg and Muir, 1989). In the long wavelength assumption, once the layered medium is deformed, such as the i th constituent medium fractured, then the fracture layer will be soft, the cross-plane strain component ε_{Ni} will enlarge, while the in-plane strains ε_T relatively are decreased or are the same as the corresponding components in the background medium with constant value. As the i th constituent relative thickness h_f approaches zero, the expression $\sigma_N = \overline{c_{NT}} \varepsilon_T + \overline{c_{NN}} \varepsilon_N$ (Figure1) is approximated to describe the relation of the stress and strain for a fracture, $\sigma_{Nf} \approx \overline{c_{NNf}} \varepsilon_{Nf}$ (Cui et al., 2012). It turns out that the fracture effects rely on modulus matrix (stiffness) c_{NNf} , which is related to on-plane stress and cross-plane strain of the fracture. There are the six independent components but only 2 of the non- negative parameters in the matrix will describe the characters of the fracture if the fractured medium is a transversely isotropic

medium (TI). Let $\overline{c_{NNf}^{-1}} = \mathbf{z} = \begin{bmatrix} z_N & 0 & 0 \\ 0 & z_T & 0 \\ 0 & 0 & z_T \end{bmatrix}$ for VTI medium. Here z_N and z_T are normal and tangential compliances of an average fracture of dimension length/stress (Schoenberg and Douma, 1988) respectively. Furthermore, the components of z in the plane of interface are equal. i.e. $c_{44} = c_{55}$. If the width of the fracture does not approach zero and has nothing to infill the space, the fracture behavior will still exhibit linear action. Consider the width of the fracture layer as H_f , with the relative thickness as h_f respect to the medium thickness H , then $H_f = h_f H$. So the fracture layer moduli should be $c_{NNf} =$

$h_f c_{NN}$, $c_{TNf} = h_f c_{TN}$, $c_{Tff} = h_f c_{TT}$, where c_{NN} , c_{TN} , and c_{TT} are elastic moduli of the media with thickness H . So the fracture moduli (Figure 2) are

$$c_{11} = c_{22} = (1 + h_f^2) c_{11b} + \left[\frac{2h_f}{c_{33b} z_N} - (1 + h_f^2) z_N \right] \frac{c_{13}^2}{1 + c_{33} z_N},$$

$$c_{12} = c_{21} = (1 + h_f^2) c_{21b} + \left[\frac{2h_f}{c_{33b} z_N} - (1 + h_f^2) z_N \right] \frac{c_{13b}^2}{1 + c_{33b} z_N},$$

$$c_{13} = c_{31} = c_{23} = c_{32} = \frac{c_{13b}(1 + h_f)}{1 + c_{33b} z_N},$$

$$c_{33} = \frac{c_{33b}}{1 + c_{33b} z_N}, \quad c_{44} = \frac{c_{44b}}{1 + c_{44b} z_T}, \quad c_{55} = \frac{c_{55b}}{1 + c_{55b} z_T}.$$

Considering Thomsen's parameters (1986), $\epsilon = \frac{c_{11} - c_{33}}{2c_{33}}$, $\gamma = \frac{c_{66} - c_{55}}{2c_{55}}$, $E_T = \mu z_T$,

$E_N = (\lambda + 2\mu) z_N$, Then

$$E_N = \frac{2\epsilon - h_f^2}{(1 + h_f^2) \left(1 - \frac{c_{13b}^2}{c_{33b}^2} \right) + 2h_f \frac{c_{13}^2}{c_{33b}^2}}, \quad E_T = 2\gamma.$$

Here $E_T = \mu z_T$, $E_N = (\lambda + 2\mu) z_N$ are non-negative dimensionless fracture compliance that express the ratio of compliance in the fractures to the corresponding compliance in an unfractured medium. The relationship between anisotropic parameters with compliances of the fracture parameters has been established. Therefore, in a homogeneous background medium, the different width of the fracture has different fracture parameters z_N . The limit of $h_f \rightarrow 0$, will yield the elastic moduli for the transverse isotropic medium and this agrees with the solution from Schoenberg and Muir (1989) in which the fracture is modeled as a non-welded contact linear slip interface.

In 1980, Schoenberg gave a linear slip interface theory: a fracture is modeled as a non-welded contact (linear slip) interface where the particle displacements are discontinuous across the interface and the stresses are continuous across it. The particle displacements are linearly proportional to the stresses. From his pioneering work, the compliances of the fracture parameter η are elicited in the boundary condition. For example, in the VTI medium, if one horizontal fracture can be modeled as a horizontal non-welded interface, then

$$\begin{aligned} \boldsymbol{\varphi}^+ - \boldsymbol{\varphi}^- &= \boldsymbol{\eta} \boldsymbol{\sigma} \\ \boldsymbol{\sigma}^- &= \boldsymbol{\sigma}^+ \end{aligned}$$

$\boldsymbol{\varphi}$ represents wave motion as u_x and u_z respectively. $\boldsymbol{\sigma}$ denotes normal (σ_{zz}) and shear (σ_{xz}) tractions of the motion. The signs of the plus and minus represent upper (left) and lower (right) medium at the interface or fracture, respectively. $\boldsymbol{\eta}$ is termed fracture parameter. η_N is normal compliance for normal incident compressional wave and η_t is tangential compliance for a normal incident shear wave. η_N and η_t are orthogonal each other. In other words, η_t is parallel to the polarization of the shear wave and perpendicular to the polarization of the compressional wave, and vice-versa for η_N . The directions of the fracture and wave polarization are very critical factors and play an integral part in the fracture forward modeling.

In 1982, Korn and Stockl presented 2D generalized homogeneous approach in which the fictitious grid points are introduced to extend one medium into the nearest-neighbor medium in order to model the SH wave propagation through a boundary. In 2000, Slawinski and Krebs used the 2D generalized homogeneous approach to model SH and P-SV wave propagation in nonwelded contact interface as a horizontal fracture. This FD scheme of wave motion with the fictitious grid points takes more physical insight into the fracture forward modeling in that the medium and boundary conditions (BCs) are imposed explicitly. In other words, the equation of motion governs the motion outside of the

discontinuity interface (fracture), but non-welded contact boundary condition is applied at the discontinuity interface. In the 2D domain, the fractures are represented as interfaces satisfying the discontinuity of displacement and continuity traction BCs across interfaces at $(x \mp 1/2, z)$, and $(x, z \mp 1/2)$ respectively.

$$\mathbf{U}_{m,n}^{t+1} = -\mathbf{U}_{m,n}^{t-1} + 2\mathbf{U}_{m,n}^t + \frac{1}{\rho} \left(\frac{\Delta t}{h} \right)^2 (\mathbf{F} \hat{\mathbf{N}} \mathbf{F} (\mathbf{U}_{m+1,n}^t - 2\mathbf{U}_{m,n}^t + \mathbf{U}_{m-1,n}^t) + \hat{\mathbf{N}} (\mathbf{U}_{m,n+1}^t - 2\mathbf{U}_{m,n}^t + \mathbf{U}_{m,n-1}^t) + \frac{1}{4} (\mathbf{F} \hat{\mathbf{G}} \mathbf{F} + \hat{\mathbf{G}}) (\mathbf{U}_{m+1,n+1}^t - \mathbf{U}_{m+1,n-1}^t - \mathbf{U}_{m-1,n+1}^t + \mathbf{U}_{m-1,n-1}^t))$$

Where $\mathbf{U}_{m,n} = \begin{bmatrix} U_{m,n}^x \\ U_{m,n}^z \end{bmatrix}$, $\mathbf{F} = \begin{bmatrix} 0 & 1 \\ 1 & 0 \end{bmatrix}$, $\hat{\mathbf{N}} = \begin{bmatrix} \frac{\mu}{1+\delta} & 0 \\ 0 & \frac{\lambda+2\mu}{1+\phi} \end{bmatrix}$, $\hat{\mathbf{G}} = \begin{bmatrix} 0 & \frac{\mu}{1+\delta} \\ \frac{\lambda}{1+\phi} & 0 \end{bmatrix}$, $\delta = \frac{z_T \mu}{h}$, $\phi = \frac{z_N (\lambda + 2\mu)}{h}$.

Examples

Obviously, There are PP and PS reflections and amplitude variation with offsets from the fractures - even though there are no impedance contrasts in the homogenous medium (Figure 1). The PP and PS amplitude are strongly affected by the direction of the fracture since waves have stronger amplitudes once their polarization direction is perpendicular to the direction of the fracture. For example, in horizontal fracture case, z-component PP wave have stronger amplitude than PS wave has (Figure 1, left) because vertical PP wave polarization is orthogonal to horizontal direction of the fracture. In the Figure 2, it is implied that seismic data are affected by fracture relative thickness. There are more effects once the direction of the wave propagation and polarization are along the normal compliance of the fractures, because fracture relative thickness only contributes to normal compliance of the fracture.

Conclusions

Note that there is no impedance contrast in the homogeneous isotropic medium, but there are still reflections that are due to the displacement discontinuity across the fracture. Any kind of fracture can be indicated by the seismic data because of the direction of the wave propagation and the plane of the fracture for normal compliance.

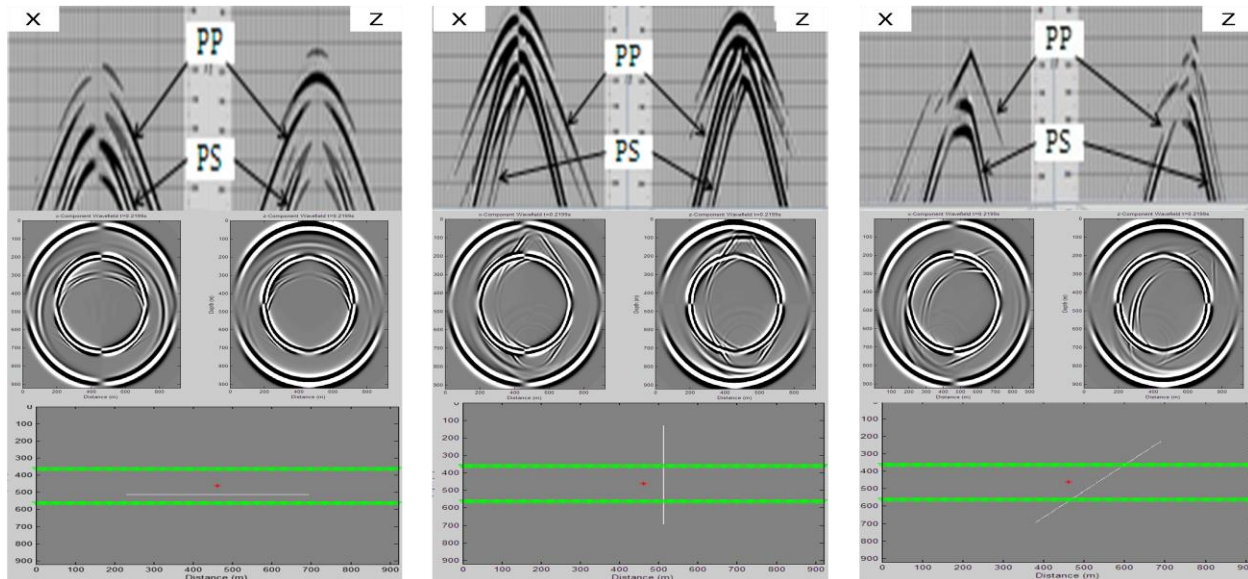


Figure 1: Horizontal (left), vertical (middle) and tilt (right) fractures model (bottom), wave field (middle) and seismograms from the fracture (top). The geometry and all parameters are described by Cui, et al. (2012)

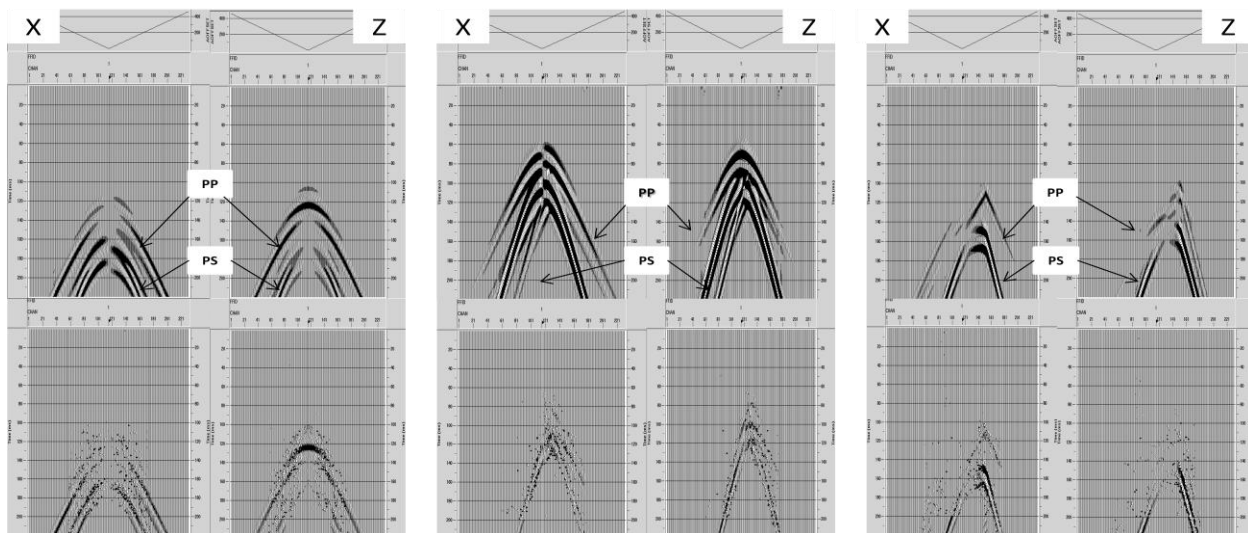


Figure 2: Horizontal (left), vertical (middle) and tilt (right) fracture seismograms. The top data simulate fracture interface relative thickness approaching to zero. The bottom shows amplitude difference of the fracture relative thickness between 0 and 0.004 (detail in CREWES Research Report (Cui, et al., 2012)).

Acknowledgments

We would like to thank the sponsors of CREWES and CHORUS. Thanks also to Ge Zhan, Zaiming Jiang and Peng Cheng for discussions of the Matlab coding.

References

- Cui, X.Q., Line, R.L., Krebs, E.S., 2012, Numerical modeling for different types of fractures: CREWES Research Report-Volume24
- Backus, G. E., 1962, Long-wave anisotropy produced by horizontal layering: J. Geophys. Res., 66, 4,427-4,440, 1962.
- Crampin, S., 1985, Evidence for aligned cracks in the Earth's crust: First Break, 3, no. 3, 12-15.
- Korn, M., and Stockl, H., 1982, Reflection and Transmission of Love Channel Wave at Coal Seam, Discontinuities Computed with a Finite Difference Method. Journal of Geophysics, 50: 171-176
- Lines, L.R., Daley, P.F., and Embleton, J.E., 2008, The resolution and detection of "subseismic" high-permeability zones in petroleum reservoirs: *The Leading Edge* May 2008 vol. 27 no. 5 664-669
- Pyrak-Nolte, L.J., L.R. Myer., and N.G.W. Cook., 1990b, Transmission of seismic wave across single natural fracture: J. Geophys. Res. 95. 8617-8638.
- Raphael A. Slawinski., and Edward S. Krebs., 2000, Finite-difference modeling of SH-wave propagation in nonwelded contact media: Geophysics. vol. 67, No5
- Schoenberg, M., 1980, Elastic wave behavior across linear slip interfaces, J. Acoust. Soc. Am., 68, 1516-1521.
- Schoenberg, M., and Douma, J., 1988, Elastic wave propagation in media with parallel fractures and aligned cracks: Geophysical Prospecting, 36, 571-590.
- Schoenberg, M., and Muir, F., 1989, A calculus for finely layered anisotropic media: Geophysics, 54, 581-589.
- Thomsen Leon., 1986, Weak elastic anisotropy: Geophysics. vol. 51, 1954-1966